A pore-expanded supramolecular organic framework and its en-richment of photosensitizers and catalysts for visible-induced hy-drogen production

Journal:	*Organic Chemistry Frontiers*
Manuscript ID	QO-RES-03-2019-000382.R1
Article Type:	Research Article
Date Submitted by the Author:	08-Apr-2019
Complete List of Authors:	Yan, Meng; Fudan University, chemistry Liu, Xu-Bo; Fudan University Gao, Zhong-Zheng; Fudan University, Chemistry Wu, Yipeng; Fudan University, Hou, Jun-Li; Department of Chemistry, Department of Chemistry Wang, Hui; Fudan University Zhang, Dan-Wei; Fudan University, Chemistry Liu, Yi; Lawrence Berkeley National Laboratory, The Molecular Foundry Li, Zhan-Ting; Fudan University, Department of Chemistry

ARTICLE

A pore-expanded supramolecular organic framework and its enrichment of photosensitizers and catalysts for visible-induced hydrogen production

Received 00th January 20xx,
Accepted 00th January 20xx

DOI: 10.1039/x0xx00000x

Meng Yan,[a] Xu-Bo Liu,[a] Zhong-Zheng Gao,[a] Yi-Peng Wu,[a] Jun-Li Hou,*[a] Hui Wang,[a] Dan-Wei Zhang,[a] Yi Liu*[b] and Zhan-Ting Li*[a]

A pore-expanded three-dimensional supramolecular organic framework **SOF-bpb**, with a previously unattained aperture size of 3.6 nm, has been constructed in water from the co-assembly of cucurbit[8]uril (CB[8]) and tetraphenylmethane-cored 1,4-bis(pyridin-4-yl)-benzene-appended building block **M1**. The periodicity of **SOF-bpb** in water and in the solid state has been confirmed by synchrotron X-ray scattering and diffraction experiments. **SOF-bpb** can adsorb anionic and neutral Ru^{2+} complex photosensitizers and anionic Wells-Dawson-type and Keggin-type polyoxometalates (POMs). The adsorption leads to important enrichment effect which remarkably increases the catalytic efficiency of the Ru^{2+} complex-POM systems for visible light-induced reduction of protons to produce H_2. The expanded aperture of **SOF-bpb** also facilitates the light absorption of the adsorbed Ru^{2+} complex photosensitizers and electron transfer between excited complexes and the POM catalysts, leading to enhanced photocatalytic activities as compared against the prototypical SOF that has an aperture size of 2.1 nm.

Introduction

Three-dimensional (3D) porous materials with aperture sizes ranging from 1 to 10 nm have attracted a lot of attentions for their promising applications as adsorption, purification, catalysis and biomedical materials.[1-3] Large pores, with internal pore diameter being >3 nm, are not only synthetic challenges that are fundamentally important, but also in principle allow for inclusion of large organic, inorganic or even biological molecules for exploring new properties or functions.[4] Currently, a variety of two-dimensional frameworks of large pores have been constructed, which can stack to form deep channels.[5] However, attempts for the preparation of large pores from long tetrahedral or octahedral building blocks often yield interpenetrating structures of diamondoid or cubic topology as a result of strong stacking of the aromatic linkers.[6]

We and others have developed the homogeneous self-assembly strategy for the generation of water-soluble supramolecular organic frameworks (SOFs) from multiarmed building blocks and cucurbit[8]uril (CB[8]),[7-15] which is driven by CB[8]-encapsulation-enhanced dimerization of appended pyridinium-derived aromatic units of the multiarmed monomers at room temperature.[16-36] The multicationic feature of the multiarmed monomers not only provide the resulting SOFs with good water-solubility, but also avoid interpenetration of the porous frameworks. We previously reported that 4-phenylpyridinium-appended tetrahedral monomers co-assemble with CB[8] to afford diamondoid SOFs that have a pore aperture of 2.1 nm.[9] We herein describe the self-assembly of a diamondoid SOF of 3.6 nm-aperture size from a 1,4-bis(pyridin-4-yl)benzene (BPB)-appended tetrahedral monomer and CB[8]. We further demonstrate that this expanded SOF is highly stable and able to simultaneously adsorb $[Ru(bpy)_3]^{2+}$-derived photosensitizers and multianionic polyoxametalate (POM) catalysts of very low concentrations, leading to enhanced efficiency of proton reduction when compared against the prototypical SOF of 2.1 nm-aperture size.

Results and discussion

Tetrahedral compound **M1** was used for the generation of the expanded 3D SOF. Within the cavity of CB[8], it was expected that fully eclipsed anti-parallel stacking of two BPB units would be disfavoured due to the electrostatic repulsion of the pyridinium units (Fig. 1).[37,38] Instead, with the encapsulation of CB[8], the slipped anti-parallel stacking was expected, which should lead to the formation of new expanded 3D framework.[39] For the synthesis of **M1** (Scheme 1), compound **3** was prepared

[a] *Department of Chemistry, Collaborative Innovation Centre of Chemistry for Energy Materials (iChEM), and Shanghai Key Laboratory of Molecular Catalysis and Innovative Materials, Fudan University, 2205 Songhu Road, Shanghai 200438, China. E-mails: houjl@fudan.edu.cn, ztli@fudan.edu.cn*
[b] *The Molecular Foundry, Lawrence Berkeley National Laboratory, One Cyclotron Road, Berkeley, California 94720, U.S.A. E-mail: yliu@lbl.gov*

† Footnotes relating to the title and/or authors should appear here.
Electronic Supplementary Information (ESI) available: Synthesis and characterization of new compounds, additional spectral, TEM and photocatalysis recycling data, ^1H and ^{13}C spectra. See DOI: 10.1039/x0xx00000x

from the reaction of **1**[40] and **2**[41] in hot DMF, which was followed by treatment with an excess of methyl iodide in MeCN under reflux. After ion exchange, **M1** was obtained as a highly water-soluble chloride salt.

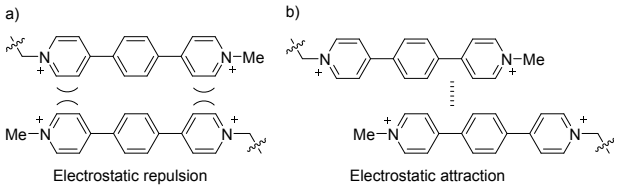

Fig. 1 a) Unfavorable eclipsed anti-parallel stacking and b) favorable slipped anti-parallel stacking patterns of the BPB units of **M1**.

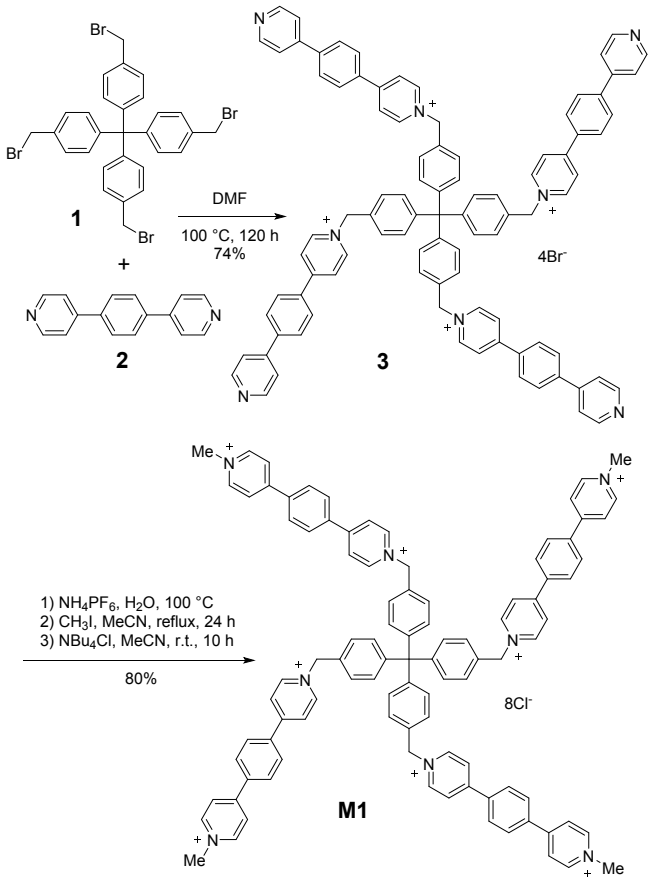

Scheme 1 The synthesis of compound **M1**.

Octacationic salt **M1** was highly water-soluble (>4.0 mM), whereas CB[8] has a very low water-solubility.[42] Mixing **M1** and CB[8] in a 1:2 molar ratio led to a homogeneous solution with the concentration of CB[8] being increased to > 2.0 mM. Similar remarkable solubilization has been observed for other reported SOFs and considered as an evidence for the formation of the framework structures. The ^{1}H NMR spectrum in D_2O showed poorly resolved peaks for both molecules (Fig. S1), indicative of substantial complexation. Previous studies showed that, for tetrahedral monomers, the appended aromatic arms selectively form 2:1 complexation with CB[8], which corresponds to a 1:2 stoichiometry.[9] The encapsulation of the appended aromatic units by CB[8] typically caused pronounced hypochromism of the former. UV–vis titration experiments revealed an inflection point for this hypochromic effect at [CB[8]]/[**M1**] = 2.0 (Fig. S2) when plotting the hypochromism of the maximum absorption (318 nm) of **M1** (1.0 mM) against [CB[8]], further confirming the 1:2 stoichiometry.[43]

Dynamic light scattering (DLS) experiments revealed the formation of large aggregates in the 1:2 solution of **M1** (1.0 mM) and CB[8] in water and the hydrodynamic diameter (D_H) of the aggregates was determined to be 94.4 nm (Fig. S3a). Upon diluting the solution to [**M1**] = 0.03 mM, the 1:2 solution still formed aggregates of D_H = 37.3 nm. In the absence of CB[8], DLS measurement afforded a D_H of 3.7 nm for the solution of **M1** (0.1 mM), reflecting significantly weaker aggregation (Fig. S3b).

Isothermal titration calorimetry (ITC) experiments were conducted by gradually adding **M1** to the aqueous solution of CB[8] (Fig. S4), from which the apparent association constant K_a for the 2:1 complexes between the two encapsulated BPB units of **M1** and CB[8] was determined to be 1.5×10^{10} M^{-2}, which was notably lower than that of the prototypical SOF with shorter 4-phenylpyridinium binding moiety, but still enabled the formation of a stable expanded SOF (vide infra, Fig. 3). The associated enthalpic (ΔH) and entropic (TΔS) contributions were −171 and −114 kJ mol^{-1}, respectively. The results indicated that the assembly of **SOF-bpb** from **M1** and CB[8] was driven enthalpically and unfavourably by entropy.[43]

Synchrotron small angle X-ray scattering (SAXS) profile for the 1:2 solution of **M1** (2.0 mM) and CB[8] revealed a discernible broad peak with the d-spacing centred around 1.83 nm (Fig. 2a). This peak matched with the calculated {400} spacing (1.83 nm) of the modelled network obtained using previously describe method,[44] supporting the formation of a new periodic water-soluble supramolecular organic framework, which we named as **SOF-bpb** to reflect the use of BPB as the appended binding unit (Fig. 3). The synchrotron SAXS profile of **SOF-bpb** microcrystals, obtained by slow evaporation of the above solution at room temperature, displayed two relatively sharper peaks centred at 1.83 and 1.49 nm (Fig. 2b), respectively, which can be assigned to the {400} and {224} facets of the modelled structure of **SOF-bpb**. The peaks were also observed on the two-dimensional synchrotron SAXS profile (Fig. 2b, inset). Synchrotron X-ray diffraction (XRD) profile of the microcrystals revealed discernible peaks with the d-spacing centred around 2.58 and 1.29 nm (Fig. 2c). The peaks matched well with the calculated {220} and {440} spacing of the modelled network. These results supported that **SOF-bpb** also maintained the ordered porosity in the solid state. Thermogravimetric analysis showed that the **SOF-bpb** microcrystals were stable at ≤ 370 °C (Fig. S5). The transmission electron microscopic (TEM) image showed a uniform bulk morphology, whereas elemental mapping analysis confirmed the compositions of the C, N, O and Cl elements (Fig. S6a).

The modelled structure of **SOF-bpb** revealed a diamondoid framework pattern. The pore aperture, which was defined by six CB[8] units in one cyclohexane-like self-assembled macrocycle, was estimated to be about 3.6 nm (Fig. 3a), which

was the largest among the reported diamondoid-type SOFs.[8d,e,9] The modelled structure of **SOF-bpb**, including the chloride anions, has approximately 85% of void volume, which is also notably larger than that (77%) of the prototypical SOFs that bear the 4-phenylpyridinium binding unit.[9]

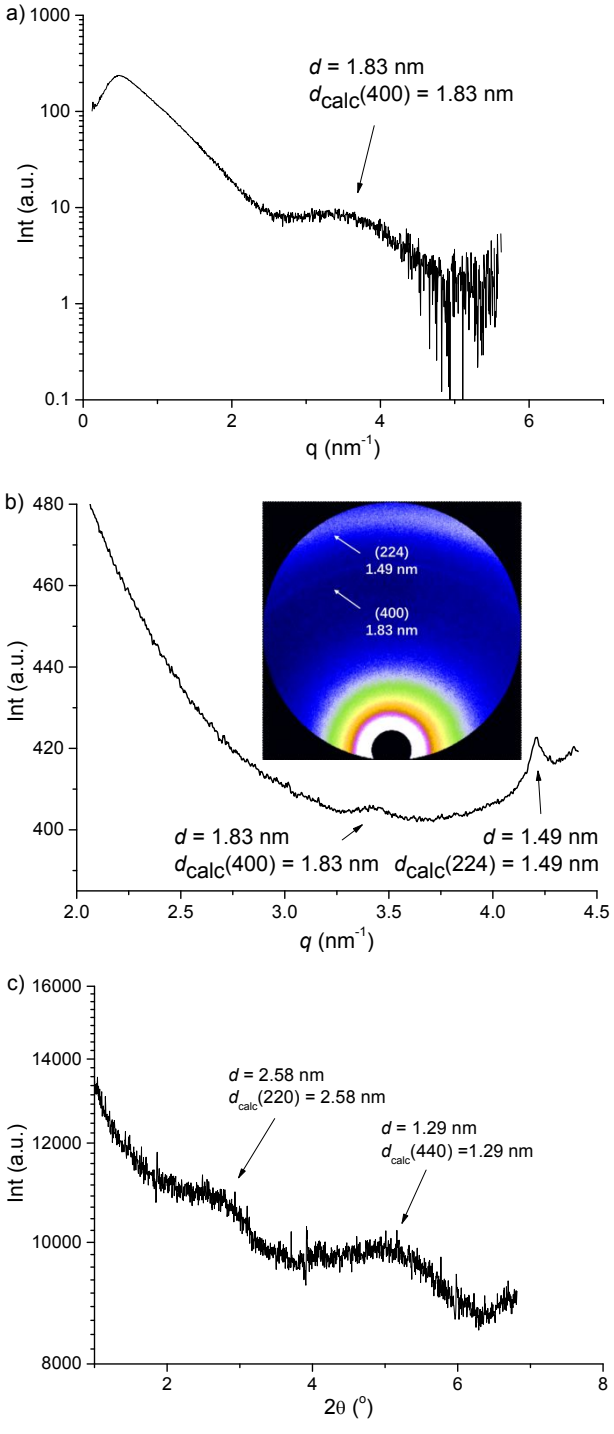

Fig. 2 a) Solution-phase synchrotron SAXS profile of **SOF-bpb** ([**M1**] = 2.0 mM). b) Solid-phase synchrotron SAXS profile of **SOF-bpb**, inset: 2D profile. c) Solid-phase synchrotron XRD profile of **SOF-bpb**. The peak values were attributed by choosing the position that was highest above the straight line defined by the two saddle points of the broad peaks.

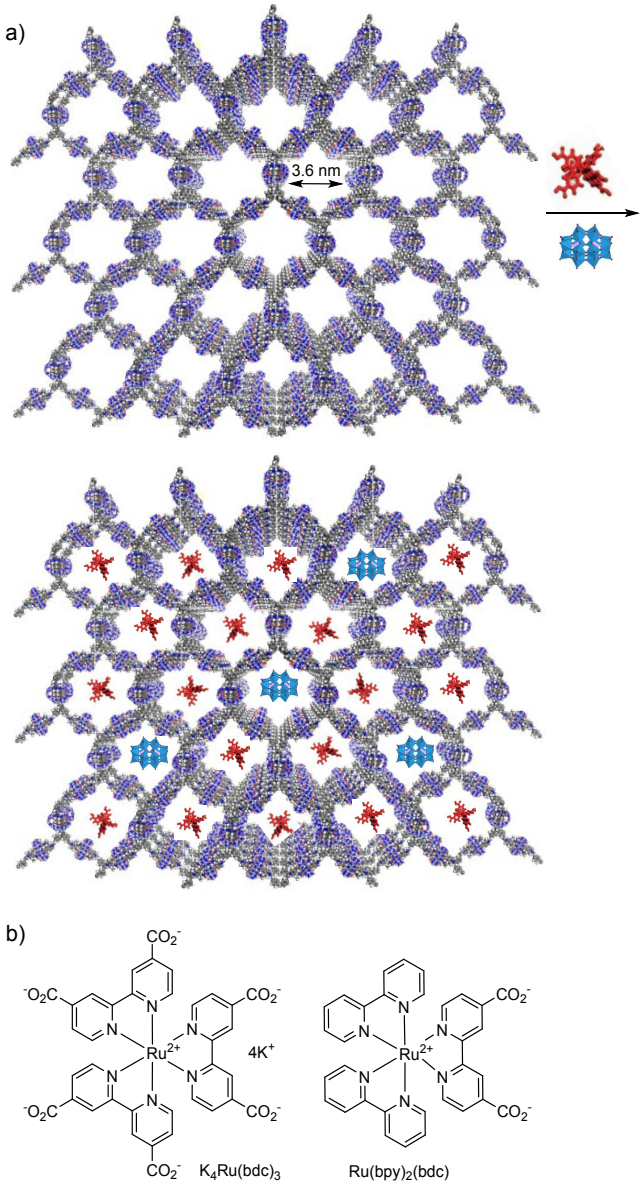

Fig. 3 a) Modelled porous structure of **SOF-bpb** and simultaneous adsorption of Ru-photosensitizer (red) and polyoxometallate catalyst (indigo). b) Structural formulas of $K_4Ru(bdc)_3$ and $Ru(bpy)_2(bdc)$).

The ability of **SOF-bpb** for the adsorption or enrichment of photosensitizers ($[Ru(bdc)^3]^{4-}$ as K^+ salt and ($Ru(bpy)_2(bdc)$) (Fig. 3b), multianionic POM catalysts (Wells-Dawson (WD)-type POM ($[P_2W_{18}O_{62}]^{6-}$ as K^+ salt and Keggin (K)-type POM ($[PW_{12}O_{40}]^{3-}$ as Na^+ salt) or their four mixtures ($K_4Ru(bdc)_3$/WD-POM (10:1), $K_4Ru(bdc)_3$/K-POM (10:1), $Ru(BPY)_2(bdc)$/WD-POM (10:1) and $Ru(bpy)_2(bdc)$/K POM (10:1)) was then investigated in water by using the fluorescence spectroscopy. All these molecular species have a size of 1.1-1.3 nm. The combination of the ruthenium complex and the polyoxometalate can constitute an integrated photocatalytic system for visible light-induced proton reduction to produce hydrogen.[8e,45,46] It was found that all these species quenched the fluorescence of **SOF-bpb** in water. Titration experiments indicated that maximum quenching was reached after about 1.6, 1.5, 1.4, or 1.8 equiv. of

the four single-component species (relative to [**M1**] in **SOF-bpb**) were added. The values corresponded to a relative ratio of 0.80, 0.38, 1.0 or 0.68 for their anion concentration over the concentration of the cation concentration of **M1** (10 μM) (Fig. S7-S10). Addition of the $K_4Ru(bdc)_3$/WD-POM (10:1), $Ru(bpy)_2(bdc)$/WD-POM (10:1), $Ru(bpy)_2(bdc)$/K-POM (10:1) or $K_4Ru(bdc)_3$/K- POM (10:1) mixtures into the solution of **SOF-bpb** also quenched the fluorescence to a comparable extent as the pure Ru^{2+} complex (Fig. S11-S14). In contrast, when adding either of the above guests or their mixtures to the solution of **M1**, fluorescence quenching was considerably less effective, highlighting the enriching effect of the **SOF-bpb** framework. This adsorption for anionic species has been rationalized by the formation of soft acid (pyridinium cation of BPB)-soft base (Ru^{2+} complexes or POMs) ion pairs and hard acid (Na^+ or K^+)-hard base (Cl^-) ion pairs.[8c] The adsorption of **SOF-bpb** for zwitterionic complex $Ru(bpy)_2(bdc)$ might be attributed to that the steric $[Ru(bpy)_3]^{2+}$ could not form efficient ion-pair interactions. As a result, the zwitterion could behave formally as a dianionic soft base. The above 10:1 ratio of the Ru^{2+} complexes/POM mixture was adapted from a related, previously optimized catalytic system that shows good catalytic activities for visible light-induced water reduction to hydrogen.[8e] Dialysis experiments for $K_4Ru(bdc)_3$ and $Ru(bpy)_2(bdc)$ (50 μM, cutoff M_n: 1000 Da) or WD-POM (50 μM, cutoff M_n: 1500 Da) in the solution of **SOF-bpb** ([**M1**] = 0.1 mM) in water revealed that, within 10 hours, no observable amount of the three guests diffused to the outside solution.[8h]

DLS revealed that, after adsorption of the ruthenium complexes and the POM salts, the four investigated **SOF-bpb** solutions afforded a D_H value that was comparable with that (53 nm) of the pure sample (Fig. S3b and S15), indicating that its porosity regularity was maintained after adsorption and no significant aggregation took place. Slow evaporation of the solution of **SOF-bpb** ([**M1**] = 0.1 mM), $K_4[Ru(bdc)_3]$ (20 μM) and WD-POM (2 μM) afforded red solid powders. Elemental mapping analysis for the microcrystals confirmed the compositions of the C, N, O, Ru, Cl, W and P elements (Fig. S6b).

Visible light (>410 nm)-induced proton reduction to produce H_2 in Ru^{2+} complex and POM-contained **SOF-bpb** solution in diluted hydrochloric water (pH = 1.8) was then investigated. DLS experiment revealed that **SOF-bpb** was stable in this acidic medium after irradiation of long time (20 h) (Fig. S3b and S15). The reactions were conducted by irradiating an 2-mL water-methanol (4:1, v/v) solution of **SOF-bpb** in the presence of different amounts of $K_4[Ru(BDC)_3]$ and WD-POM, the molar ratio of which was kept at 10:1 (Table 1), in a sealed 5-mL glass bottle. Methanol was used as sacrificial electron donor in this study. Both the ruthenium complex and POM sample were indispensable for the reduction of proton (entries 1-3, Table 1). Under all studied conditions, **SOF-bpb** exhibited remarkable enhancement effect (up to 51-fold, entry 5, Table 1) for the catalytic activity (entries 4-18, Table 1), which can be rationally attributed to its enrichment for the species and thus the increase of their effective concentration in the interior of **SOF-bpb**. This promotion effect became increasingly prominent at lowered concentrations (entries 4-10, Table 1). In particular, at the lowest concentration ($[K_4Ru(bdc)_3]$ = 2.0 μM and [WD-POM] = 0.2 μM), in the absence of **SOF-bpb**, no H_2 evolution was observed. However, with the promotion of **SOF-bpb** through the enrichment of both species, the turnover number (TON) for H_2 production reached the highest value of 781 (defined as $n(1/2H_2)/n(POM)$ (entry 4, Table 1). This value corresponded to a H_2 evolution rate, that is, turnover frequency (TOF), of 7079 μmol/g·h (based on POM), which was about two times of the highest TON achieved by the prototypical SOF that bears the short 4-phenylpyridinium binding moiety under similar conditions.[9] This increased catalytic efficiency of $([Ru(bdc)_3]^{4+}$ /WD-POM)@**SOF-bpb** system may be attributed to the decreased "density" of the Ru^{2+} complex in the expanded pores of **SOF-bpb**, which should enable better visible light absorption by the Ru^{2+} complex. The larger pores might also allow for simultaneous entrapment of both the photosensitizer and the catalyst in one diamondoid cavity, which should also facilitate electron transfer from excited Ru^{2+} complex to the "chum" POM. At $[Ru(bdc)_3]$ = 20 μM and [WD-POM] = 2 μM, gradient experiments revealed (entries 11-15, Table 1) that, at [**M1**] = 0.1 mM, **SOF-bpb** caused the highest TON, which decreased notably at higher concentration of the framework, which may be ascribed to the decrease of light transmittance of the solution. At [**M1**] = 0.1 mM, **SOF-bpb** also enhanced the catalytic efficiency of the $K_4Ru(bdc)_3$/K-POM, $Ru(BPY)_2(bdc)$/ WD-POM and $Ru(bpy)_2(bdc)$/K-POM combinations (entries 16-18, Table 1) and the related TON values were even higher than that of the $K_4Ru(bdc)_3$/WD-POM combination. Control experiment revealed that, in the absence of CB[8], **M1** (0.1 mM) did not produce any observable promotion effect, because the resulting TON (49) was exactly the same as that in the absence of **SOF-bpb** (entry 8, Table 1).

Table 1 Enhanced hydrogen evolution in the solution of **SOF-bpb** in water and methanol (4:1, v/v, pH = 1.8 with HCl) containing Ru^{2+} complex photosensitizers and POM catalysts[a)]

Entry	[**M1**] (mM)	Ru^{2+} (μM)	POM (μM)	**TON-1** [f)]	**TON-2** [g)]	**TON-1 /TON-2**
1	0.1	A (20)	C (0)	0	0	-
2	0.1	A (0)	C (2.0)	0	0	-
3	0.1	B (20)	D (0)	0	0	-
4	0.1	A [b)] (2.0)	C [d)] (0.2)	781	0	-
5	0.1	A (6.0)	C (0.6)	763	15	51
6	0.1	A (10)	C (1.0)	429	26	17
7	0.1	A (16)	C (1.6)	475	51	9
8	0.1	A (20)	C (2.0)	505	49	10
9	0.1	A (26)	C (2.6)	367	41	9
10	0.1	A (30)	C (3.0)	316	37	9
11	0.01	A (20)	C (2.0)	117	49	3
12	0.05	A (20)	C (2.0)	257	49	5
13	0.1	A (20)	C (2.0)	352	49	7
14	0.15	A (20)	C (2.0)	272	49	6
15	0.2	A (20)	C (2.0)	246	49	5
16	0.1	A (20)	D [e)] (2.0)	634	43	15
17	0.1	B [c)] (20)	C (2.0)	608	45	14
18	0.1	B (20)	D (2.0)	599	38	16

a) Irradiation time = 20 h, b) A = $K_4Ru(bdc)_3$, c) B = $Ru(bpy)_2(bdc)$, d) C = Wells-Dawson-type POM, e) D = Keggin-type POM, f) in the presence of **SOF-bpb**, and g) without **SOF-bpb**.

Irradiating the solution for longer time (20-70 hours) still led to H_2 evolution, even though the efficiency became increasingly lower (Fig. S16). When the solution was left to stand for some time, typically 12 hours, the catalytic activity of the system recovered to a considerable extent. In this way, the solution could be irradiated for ten times (Table 2) to produce H_2, albeit with a decreasing efficiency. Control experiments showed that, in the absence of **SOF-bpb**, irradiating the solution of $K_4[Ru(BDC)_3]$ and WD-POM could also produce H_2 and this process could be conducted for four times after repeated standing. However, the catalytic efficiency was generally substantially lower (entries 1-4, Table 2). These results not only confirmed the enrichment effect of **SOF-bpb**, but also suggested that the enrichment increased the efficiency and stability of the bi-component catalytic system, which might be attributed to the fact that adsorption could decrease the aggregation of the photosensitizer and catalyst molecules.[47] DLS experiment for the **SOF-bpb** solutions after long time and repeated irradiation afforded D_H that was comparable to that of the originally prepared sample (Fig. S15), supporting that the frameworks still maintained their integrity to enable continued enrichment effect.

Table 2 Hydrogen evolution in the solution of **SOF-bpb** (0.1 mM) in water and methanol (4:1, v/v, pH = 1.8 with HCl) containing $K_4Ru(bdc)_3$ (20 μM) and Wells-Dawson-POM (2.0 μM)[a)]

Entry	TON-1	TON-2 [b)]	TON-1/TON-2
1	506	49	10
2	499	32	16
3	475	25	19
4	400	13	31
5	396	-	-
6	362	-	-
7	312	-	-
8	272	-	-
9	258	-	-
10	225	-	-

a) Irradiation time = 20 h, b) without **SOF-bpb**.

Conclusions

We have demonstrated the construction of a 3.6 nm-aperture 3D SOF by elongating the peripheral aromatic binding moiety of the tetrahedral building block. The new pore-expanded SOF exhibits very strong adsorption ability for Ru^{2+} complex photosensitizers and POM, which remarkably promotes their visible light-initiated photocatalysis for the proton reduction to produce hydrogen. The new SOF is highly stable to allow for repeated use and its expanded pore size enables increased light absorption and/or photosensitizer-to-catalyst electron transfer and thus leads to higher catalysis efficiency as compared against that of the prototypical SOF of smaller pore size. The good water-solubility and high stability of this 3.6 nm-aperture SOF bodes well for the generation of new SOFs of the same topology that possess even larger aperture for the encapsulation and delivery of biomacromolecules such as proteins.

Conflicts of interest

There are no conflicts to declare.

Acknowledgements

This work was supported by National Natural Science Foundation of China (21432004, 21529201 and 21890732). YL thanks the support from the Molecular Foundry, a national user facility supported by the Office of Science, Office of Basic Energy Sciences, of the U.S. Department of Energy under Contract No. DE-AC02-05CH11231. We are also grateful for Shanghai Synchrotron Radiation Facility (beamlines BL16B1 and BL14B1) for providing the beam time. Solution SAXS studies were conducted at the SIBYLS Beamline 12.3.1 of the Advanced Light Source (ALS), a national user facility supported by Department of Energy, Office of Basic Energy Sciences, through the Integrated Diffraction Analysis Technologies (IDAT) program, supported by DOE Office of Biological and Environmental Research. Additional support comes from the National Institute of Health project ALS-ENABLE (P30 GM124169) and a High-End Instrumentation Grant S10OD018483.

Notes and references

1 P. Liu and G. F. Chen, (Eds.) *Porous Materials: Processing and Applications*, Oxford: Butterworth-Heinemann Publisher, 2014.
2 L. R. MacGillivray and C. M. Lukehart, (Eds.) *Metal-Organic Framework Materials*, Chichester: John Wiley & Sons, 2015.
3 G. Zhu and H. Ren, (Eds.) *Porous Organic Frameworks: Design, Synthesis and Their Advanced Applications*, Berlin: Springer-Verlag, 2015.
4 (*a*) L. Ma, J. M. Falkowski, C. Abney and W. Lin, *Nat. Chem*., 2010, **2**, 838–846; (*b*) G. Liu, J. Sheng and Y. Zhao, *Sci. China Chem*., 2017, **60**, 1015–1022; (*c*) L. Cao, T. Wang and C. Wang, *Chin. J. Chem*., 2018, **36**, 754–764; (*d*) D. Liu, D. Zou, H. Zhu and J. Zhang, *Small*, 2018, **14**, 1801454; (*e*) Y. Song, Q. Sun, B. Aguila and S. Ma, *Adv. Sci*., 2019, **6**, 1801410; (*f*) R.-R. Liang and X. Zhao, *Org. Chem. Front*., 2018, **5**, 3341–3356; (*g*) X. Zhao, Z. Zhang, X. Cai, B. Ding, C. Sun, G. Liu, C. Hu, S. Shao and M. Pang, *ACS Appl. Mater. Interf*., 2019, **11**, 7884–7892.
5 (*a*) H. Deng, S. Grunder, K. E. Cordova, C. Valente, H. Furukawa, M. Hmadeh, F. Gándara, A. C. Whalley, Z. Liu, S. Asahina, H. Kazumori, M. O'Keeffe, O. Terasaki, J. F. Stoddart and O. M. Yaghi, *Science*, 2012, **366**, 1018–1023; (*b*) S. Jin, K. Furukawa, M. Addicoat, L. Chen, S. Takahashi, S. Irle, T. Nakamura and D. Jiang, *Chem. Sci*., 2013, **4**, 4505–4511; (*c*) Q. Fang, Z. Zhuang, S. Gu, R. B. Kaspar, J. Zheng, J. Wang, S. Qiu and Y. Yan, *Nat. Commun*., 2014, **5**, 4503; (*d*) H. Yang, Y. Du, S. Wan, G. D. Trahan, Y. Jin and W. Zhang, *Chem. Sci*., 2015, **6**, 4049–4053; (*e*) Y. Zhang, T.-G. Zhan, T.-Y. Zhou, Q.-Y. Qi, X.-N. Xu and X. Zhao, *Chem. Commun*., 2016, **52**, 7588–7591; (*f*) L. Zhang, Y. Jia, H. Wang, D.-W. Zhang, Q. Zhang, Y. Liu and Z.-T. Li, *Polym. Chem*., 2016, **7**, 1861–1865.

6 (*a*) B.-Q. Song, X.-L. Wang, G.-S. Yang, H.-N. Wang, J. Liang, K.-Z. Shao and Z.-M. Su, CrystEngComm, 2014, 16, 6882–6888; (*b*) M. Frank, M. D. Johnstone and G. H. Clever, *Chem. Eur. J.*, 2016, **22**, 14104–14125; (*c*) G. Lin, H. Ding, R. Chen, Z. Peng, B. Wang and C. Wang, *J. Am. Chem. Soc.*, 2017, **139**, 8705–8709; (*d*) T. Ma, E. A. Kapustin, S. X. Yin, L. Liang, Z. Zhou, J. Niu, L. H. Li, Y. Wang, J. Su, J. Li, X. Wang, W. D. Wang, W. Wang, J. Sun and O. M. Yaghi, *Science*, 2018, **361**, 48–52; (*e*) H. Ding, G. Xie, G. Lin, R. Chen, Z. Peng, C. Yang, B. Wang, C. Wang, J. Li and J. Sun, *Nat. Commun.*, 2018, **9**, 5234.

7 (*a*) J. Tian, H. Wang, D.-W. Zhang, Y. Liu and Z.-T. Li, *Natl. Sci. Rev.*, 2017, **4**, 426–436; (*b*) Y. Chen, F. Huang, Z.-T. Li and Y. Liu, *Sci. China Chem.*, 2018, **61**, 979–992.

8 (*a*) K.-D. Zhang, J. Tian, D. Hanifi, Y. Zhang, A. C. H. Sue, T.-Y. Zhou, L. Zhang, X. Zhao, Y. Liu and Z.-T. Li, *J. Am. Chem. Soc.*, 2013, **135**, 17913–17918; (*b*) L. Zhang, T.-Y. Zhou, J. Tian, H. Wang, D.-W. Zhang, X. Zhao, Y. Liu and Z.-T. Li, *Polym. Chem.*, 2014, **5**, 4715–4721; (*c*) J. Tian, Z.-Y. Xu, D.-W. Zhang, H. Wang, S.-H. Xie, D.-W. Xu, Y.-H. Ren, H. Wang, Y. Liu and Z.-T. Li, *Nat. Commun.*, 2016, **7**, 11580; (*d*) Y.-P. Wu, B. Yang, J. Tian, S.-B. Yu, H. Wang, D.-W. Zhang, Y. Liu and Z.-T. Li, *Chem. Commun.*, 2017, **53**, 13367–13370; (*e*) S.-B. Yu, Q. Qi, B. Yang, H. Wang, D.-W. Zhang, Y. Liu and Z.-T. Li, *Small*, 2018, **14**, 1801037; (*f*) C. Yao, J. Tian, H. Wang, D.-W. Zhang, Y. Liu, F. Zhang and Z.-T. Li, *Chin. Chem. Lett.*, 2017, **28**, 893–899; (*g*) X.-F. Li, S.-B. Yu, B. Yang, J. Tian, H. Wang, D.-W. Zhang, Y. Liu and Z.-T. Li, *Sci. China Chem.*, 2018, **61**, 830–835; (*h*) J. Tian, C. Yao, W.-L. Yang, L. Zhang, D.-W. Zhang, H. Wang, F. Zhang, Y. Liu and Z.-T. Li, *Chin. Chem. Lett.*, 2017, **28**, 798–806.

9 J. Tian, T.-Y. Zhou, S.-C. Zhang, S.-H. Xie, D.-W. Zhang, X. Zhao, Y. Liu and Z.-T. Li, *Nat. Commun.*, 2014, **5**, 5574.

10 (*a*) S.-Q. Xu, X. Zhang, C.-B. Nie, Z.-F. Pang, X.-N. Xu and X. Zhao, *Chem. Commun.*, 2015, **51**, 16417–16420; (*b*) S.-Y. Jiang and X. Zhao, *Chin. J. Polym. Sci.*, 2019, **37**, 1–10.

11 M. Pfeffermann, R. Dong, R. Graf, W. Zajaczkowski, T. Gorelik, W. Pisula, A. Narita, K. Müllen and X. Feng, *J. Am. Chem. Soc.*, 2015, **137**, 14525–14532.

12 Y. Li, Y. Dong, X. Miao, Y. Ren, B. Zhang, P. Wang, Y. Yu, B. Li and L. Isaacs and L. Cao, *Angew. Chem. Int. Ed.*, 2018, **57**, 729–733.

13 H.-J. Lee, H.-J. Kim, E. C. Lee, J. Kim and S.-Y. Park, *Chem. Asian J.*, 2018, **13**, 390–394.

14 K. Madasamy, V. M. Shanmugam, D. Velayutham, M. Kathiresan, K. Madasamy, D. Velayutham and M. Kathiresan, *Sci. Rep.*, 2018, **8**, 1354.

15 H. Liu, Z. Zhang, Y. Zhao, Y. Zhou, B. Xue, Y. Han, Y. Wang, X. Mu, S. Zang, X. Zhou and Z. Li, *J. Mater. Chem. B*, 2019, **7**, 1435–1441.

16 Y.-H. Ko, E. Kim, I. Hwang and K. Kim, *Chem. Commun.*, 2007, 1305–1315.

17 L. Isaacs, *Chem. Commun.*, 2009, 619–629.

18 Y. Liu, H. Yang, Z. Wang and X. Zhang, *Chem. Asian J.*, 2013, **8**, 1626–1632.

19 F. Biedermann, W. M. Nau and H.-J. Schneider, *Angew. Chem. Int. Ed.*, 2014, **53**, 11158–11171.

20 T.-Y. Zhou, Q.-Y. Qi, Y. Zhang, X.-N. Xu and X. Zhao, *Org. Chem. Front.*, 2015, **2**, 1030–1034.

21 Q. Zhang, D.-H. Qu, Q.-C. Wang and H. Tian, *Angew. Chem. Int. Ed.*, 2015, **54**, 15789–15793.

22 S. J. Barrow, S. Kasera, M. J. Rowland, J. del Barrio and O. A. Scherman, *Chem. Rev.*, 2015, **115**, 12320–12406.

23 J. Tian, L. Chen, D.-W. Zhang, Y. Liu and Z.-T. Li, *Chem. Commun.*, 2016, **52**, 6351–6362.

24 J. Liu, Y. Lan, Z. Yu, C. S. Y. Tan, R. M. Parker, C. Abell and O. A. Scherman, *Acc. Chem. Res.*, 2017, **50**, 208–217.

25 Z.-Y. Xiao, R.-L. Lin, Z. Tao, Q.-Y. Liu, J.-X. Liu and X. Xiao, *Org. Chem. Front.*, 2017, **4**, 2422–2427.

26 C. Stoffelen, E. Staltari-Ferraro and J. Huskens, *J. Mater. Chem. B* 2015, **3**, 6945–6952.

27 L. M. Heitmann, A. B. Taylor, P. J. Hart and A. R. Urbach, *J. Am. Chem. Soc.*, 2006, **128**, 12574–12581.

28 S. Wu, J. Li, H. Liang, L. Wang, X. Chen, G. Jin, X. Xu and H.-H. Yang, *Sci. China Chem.*, 2017, **60**, 628–634.

29 R. Wang, S. Qiao, L. Zhao, C. Hou, X. Li, Y. Liu, Q. Luo, J. Xu, H. Li and J. Liu, *Chem. Commun.*, 2017, **53**, 10532–10535.

30 Q. Li, J. Sun, J, Zhou, B. Hua, L. Shao and F. Huang, *Org. Chem. Front.*, 2018, **5**, 1940–1944.

31 Z.-J. Yin, Z.-Q. Wu, F. Lin, Q.-Y. Qi, X.-N. Xu and X. Zhao, *Chin. Chem. Lett.*, 2017, **28**, 1167–1171.

32 H. Zou, J. Liu, Y. Li, X. Li and X. Wang, *Small*, 2018, **14**, 1802234.

33 K. Kotturi and E. Masson, *Chem. Eur. J.*, 2018, **24**, 8670–8678.

34 X.-M. Chen, Y. Chen, Q. Yu, B.-H. Gu and Y. Liu, *Angew. Chem. Int. Ed.*, 2018, **57**, 12519–12523.

35 W. Xu, J. Kan, B. Yang, T. J. Prior, B. Bian, X. Xiao, Z. Tao and C. Redshaw, *Chem. Asian J.*, 2019, **14**, 235–242.

36 E. Pazos, P. Novo, C. Peinador, A. E. Kaifer and M. D. Garcia, *Angew. Chem. Int. Ed.*, 2019, **58**, 403–416.

37 G. Wu, M. Olesinska, Y. Wu, D. Matak-Vinkovic and O. A. Scherman, *J. Am. Chem. Soc.*, 2017, **139**, 3202–3208.

38 B. Yang, S.-B. Yu, H. Wang, D.-W. Zhang and Z.-T. Li, *Chem. Asian J.*, 2018, **13**, 1312–1317.

39 Y. Zhang, T.-Y. Zhou, K.-D. Zhang, J.-L. Dai, Y.-Y. Zhu and X. Zhao, *Chem. Asian J.*, 2014, **9**, 1530–1534.

40 J. Tian, Y.-D. Ding, T.-Y. Zhou, K.-D. Zhang, X. Zhao, H. Wang, D.-W. Zhang, Y. Liu and Z.-T. Li, *Chem. Eur. J.*, 2014, **20**, 575–584.

41 Y.-S. Su and C.-F. Chen, *Org. Lett.*, 2010, **12**, 1888–1891.

42 J. Lagona, P. Mukhopadhyay, S. Chakrabarti and L. Isaacs, *Angew. Chem. Int. Ed.*, 2005, **44**, 4844–4870.

43 (*a*) L. M. Heitmann, A. B. Taylor, P. J. Hart and A. R. Urbach, *J. Am. Chem. Soc.*, 2006, **128**, 12574–12581; (*b*) Z. Huang, L. Yang, Y. Liu, Z. Wang, O. A. Scherman and X. Zhang, *Angew. Chem. Int. Ed.*, 2014, **53**, 5351–5355.

44 Accelrys Materials Studio Release Notes, Release 7.0, Accelrys Software Inc., San Diego, USA, 2013 (accessed: December 2013) https://www.scientific-computing.com/press-releases/accelrys-materials-studio-70

45 (*a*) K. Zeitler, *Angew. Chem. Int. Ed.*, 2009, **48**, 9785–9789; (*b*) L.-L. Mao, D.-G. Zheng, X.-H. Zhu, A.-X. Zhou and S.-D. Yang, *Org. Chem. Front.*, 2018, **5**, 232–236.

46 (*a*) R. Sivakumar, J. Thomas and M. Yoon, J. Photochem. Photobiol. C, 2012, 13, 277–298; (*b*) H. Lv, J. Song, H. Zhu, Y. V. Geletii, J. Bacsa, C. Zhao, T. Lian, D. G. Musaev and C. L. Hill, J. Catal., 2013, 307, 48–54; (*c*) Z.-M. Zhang, T. Zhang, C. Wang, Z. Lin, L.-S. Long and W. Lin, *J. Am. Chem. Soc.*, 2015, **137**, 3197–3200.

47 (*a*) K. Mori, T. Hara, T. Mizugaki, K. Ebitani and K. Kaneda, *J. Am. Chem. Soc.*, 2004, **126**, 10657–10666; (*b*) W. Gan, P. J. Dyson and G. Laurenczy, *ChemCatChem*, 2013, **5**, 3124–3130; (*c*) D. Astruc, F. Lu and J. R. Aranzaes, *Angew. Chem. Int. Ed.*, 2005, **44**, 7852–7872.